

Conf -930907--6

UCRL-JC-113528
PREPRINT

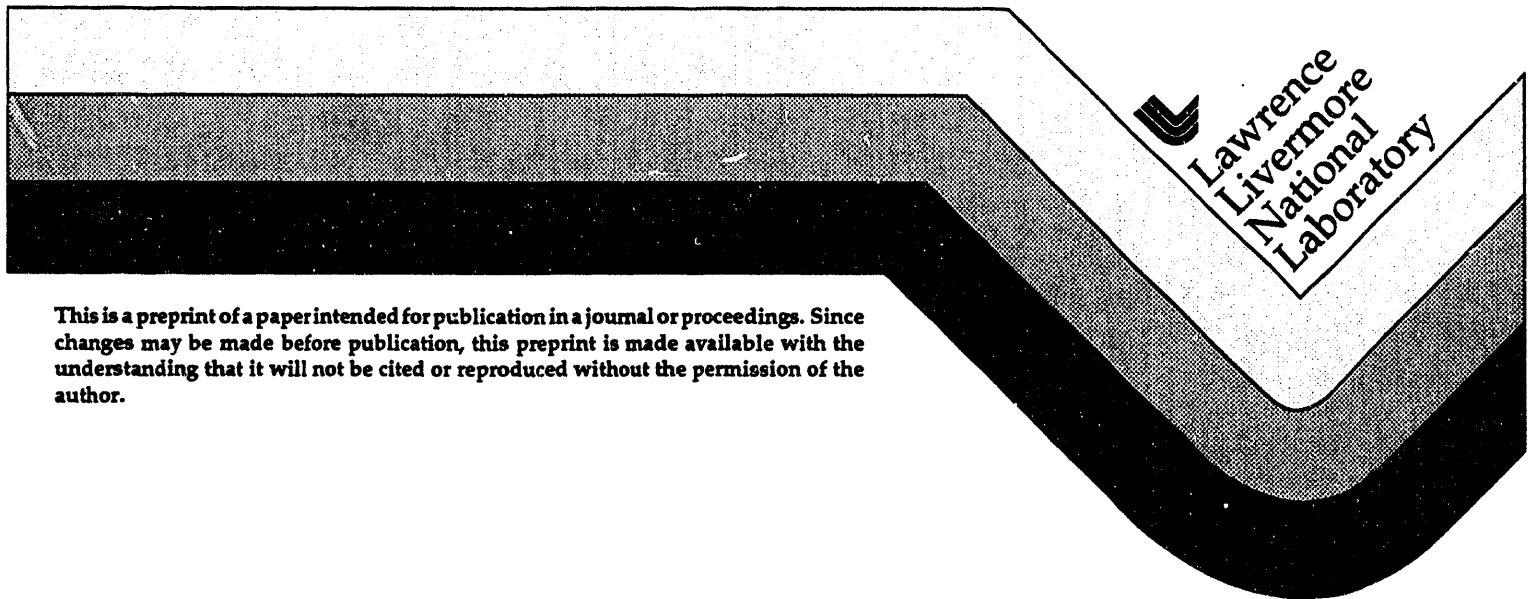
RECEIVED
JUL 16 1993
OSTI

The Dissolver Paradox as a Coupled Fast-Thermal Reactor

Harry F. Lutz
Paul S. Webb

This paper was prepared for submittal to
1993 Topical Meeting on Physics and Methods in Criticality Safety
Nashville, TN
September 19-23, 1993

May 1993



This is a preprint of a paper intended for publication in a journal or proceedings. Since changes may be made before publication, this preprint is made available with the understanding that it will not be cited or reproduced without the permission of the author.

MASTER

DISTRIBUTION OF THIS DOCUMENT IS UNLIMITED

ds

DISCLAIMER

This document was prepared as an account of work sponsored by an agency of the United States Government. Neither the United States Government nor the University of California nor any of their employees, makes any warranty, express or implied, or assumes any legal liability or responsibility for the accuracy, completeness, or usefulness of any information, apparatus, product, or process disclosed, or represents that its use would not infringe privately owned rights. Reference herein to any specific commercial products, process, or service by trade name, trademark, manufacturer, or otherwise, does not necessarily constitute or imply its endorsement, recommendation, or favoring by the United States Government or the University of California. The views and opinions of authors expressed herein do not necessarily state or reflect those of the United States Government or the University of California, and shall not be used for advertising or product endorsement purposes.

The Dissolver Paradox as a Coupled Fast-Thermal Reactor

by
Harry F. Lutz
Lawrence Livermore National Laboratory
and
Paul S. Webb
MHC Associates

The dissolver paradox is treated as coupled fast-thermal reactors. Each reactor is sub-critical but the coupling is sufficient to form a critical system. The practical importance of the system occurs when the fast system by itself is mass limited and the thermal system by itself is volume limited. Numerous 1D calculations have been made to calculate the neutron multiplication parameters of the separate fast and thermal systems that occur in the dissolver paradox. A model has been developed to describe the coupling between the systems. Monte Carlo calculations using the MCNP code have tested the model.

Introduction

In this paper we report a series of calculations that were intended to provide insight for the dissolver paradox¹. The dissolver paradox is of some practical importance to the criticality safety specialist because it shows how critical systems can be made when a solid metal system is limited by mass and a solution system is limited by volume. The subcritical fast and thermal systems couple together to form a critical system. The system we consider is a sphere of metallic plutonium (19.7 g/cc ²³⁹Pu) surrounded by a plutonium metal-water mixture, which is in turn surrounded by a thick water reflector. We label the components of this system cells 1, 2 and 3. We perform calculations on three configurations. Configuration "a" is the entire critical system. Configuration "b" is just the metal pit with a thick water reflector. Configuration "c" is the metal-water mixture with a void instead of the metal pit, also surrounded by a thick water reflector.

For interpretive purposes, we start by reviewing some seminal work on coupled reactors by Avery². We then describe some multigroup discrete ordinates transport (SAN version of ANISN³) calculations that determined the parameters of critical systems consisting of plutonium metal spheres of various sizes surrounded by a plutonium metal-water mixtures of various concentrations, which are in turn surrounded by a thick water reflector. Finally the parameters

determined by the SAN calculations were used to set up MCNP4 problems that employed flagged tallies.

Review of Avery's Coupled Reactor Theory

From Avery², the condition for two subcritical systems to form a critical coupled system is:

$$k_{12} k_{21} = \Delta_1 \Delta_2 . \quad (1)$$

k_{12} is defined as the expectation value that a fission neutron in reactor 2 gives rise to a next generation fission neutron in reactor 1. k_{21} is defined as the expectation value that a fission neutron in reactor 1 gives rise to a next generation fission neutron in reactor 2.

The degree of subcriticality is given by:

$$\Delta = 1 - k_{eff} . \quad (2)$$

k_{eff} , k_{∞} and the net neutron leakage probability, p_L , are related by:

$$k_{eff} = k_{\infty} (1 - p_L) . \quad (3)$$

Solving for p_L gives:

$$p_L = 1 - \frac{k_{eff}}{k_{\infty}} . \quad (4)$$

At critical, Avery shows that the ratio of the total fission neutron source in reactor 1 to that in reactor 2 is given by:

$$\frac{S_1}{S_2} = \frac{k_{12}}{\Delta_1} = \frac{\Delta_2}{k_{21}} . \quad (5)$$

We can propose simple analytic expressions for k_{21} and k_{12} which can be compared with the values determined using equation (5) and MCNP calculations. In the particular system we consider, all neutrons leaking from cell 1 (the metal core) enter cell 2 (the metal-water mixture).

$$\begin{aligned}
k_{21} &\approx P_{L,1} k_{eff,2} \\
&\approx \left(1 - \frac{k_{eff,1}}{k_{\infty,1}}\right) k_{eff,2}
\end{aligned} \tag{6}$$

Neutrons that leak from cell 2 (metal-water mixture) can either enter cell 1 or go into the water reflector that surrounds the system. Assume, for the moment, that neutrons in the water reflector are not likely to return to system 1. If we further assume that the fraction of neutrons leaking from cell 2 to cell 1 is proportional to the ratio of the area of the inner surface to the total surface area of the metal-water mixture, we can write:

$$\begin{aligned}
k_{12} &\approx P_{L,2} \left(\frac{R_{<}}{R_{<} + R_{>}}\right)^2 k_{eff,1} \\
&\approx \left(1 - \frac{k_{eff,2}}{k_{\infty,2}}\right) \left(\frac{R_{<}}{R_{<} + R_{>}}\right)^2 k_{eff,1}
\end{aligned} \tag{7}$$

where $R_{<}$ is the radius of the inner surface and $R_{>}$ is the radius of the outer surface.

Equations (6) and (7) indicate that k_{21} will be greater than k_{12} because of the factor involving the ratio of the inner surface to the total surface in Equation (7).

According to Equation (6) the value for k_{21} decreases as the radius of the metal pit increases and the thickness of the metal-water cell decreases. This is reasonable because the pit becomes less leaky and the multiplication of the thinner metal-water solution also decreases. According to Equation (7) the value for k_{12} increases as the radius of the metal pit increases and the thickness of the metal water decreases. The fraction of the neutrons crossing the inner surface increases as the thickness of the metal-water cell decreases, and the multiplication of the metal pit increases.

SAN Calculations

SAN, which is an LLNL version of ANISN³, multigroup calculations were performed to obtain the dimensions of critical systems consisting of spheres of metallic plutonium with masses from 1 kg to 4.5 kg in 0.5 kg steps and plutonium metal-water mixtures with densities 0.032, 0.1, 0.2, 0.3, and 0.4 g/cc. A 30 cm

thick reflector surrounded the system. For each value of mass of solid pit and density of metal-water mixture, the thickness of the metal-water mixture was varied until the system was critical. K-effective for a system consisting only of the metal pit with a water reflector was calculated and called k_{b_1} , for configuration "b" cell 1. Then the value for k-effective for a system consisting of the metal-water mixture with a void instead of the pit was calculated and called k_{c_2} , for configuration "c" cell 2. The results of the calculations are summarized in Table 1. The critical systems considered in this paper can have masses as low as 1.37 kg ^{239}Pu and volumes of the fuel region as low as 1.14 liters.

MCNP Calculations

The calculations made with the MCNP used the same dimensions as the SAN calculations. No attempt was made to modify dimensions to obtain a k_{eff} of unity.

The values of k_{eff} obtained with the MCNP calculations varied from 0.986 to 1.0026.

As with the SAN calculations, 3 configurations were modeled: configuration "a" being the entire critical system; configuration "b" being the metal pit surrounded by a water reflector; configuration "c" being the metal-water mixture with a void instead of a metal pit. MCNP gave values of k_{b_1} slightly higher than the SAN results. For concentrations less than 0.3 g/cc, MCNP gave slightly lower values of k_{c_2} than the SAN results. For concentrations greater than 0.3 g/cc, MCNP gave slightly higher values of k_{c_2} than the SAN results.

The MCNP calculations made use of the flagged tallies feature of the code. In our case we determined a track-length estimate of k-effective in which neutrons were flagged by the cells in which they had traveled. We refer to the pit as cell 1, the metal-water mixture as cell 2 and the water reflector as cell 3. Hence the column labeled k_{a_1} in Table 2 is the k-effective value for cell 1 in the complete system. The column labeled $k_{a_1:2}$ is the k-effective value for cell 1 due to neutrons that have been in cell 2. $k_{a_1:2}$ is not the same as k_{12} which refers to neutrons born in cell 2. Some sort of double counting can occur in the flagged tallies. For example in system-a, cell 2 there are cases where the sum of $k_{a_2:1}$ and $k_{a_2:3}$ exceed k_{a_2} . This is due to neutrons from the solid pit going through the solution and scattering back to the solution from the reflector. Note that the solution cell is always the critical part of the system. This may be due to the way the SAN calculations varied the solution cell configuration until the system was critical.

In Table 3 we show the results for k_{12} and k_{21} using equation (5) and the MCNP calculations. We see that k_{21} , the expectation value that a fission neutron in the metal pit gives rise to a next generation fission neutron in the solution, is always much larger than k_{12} . This result shows that it is neutrons from the solid pit that drive the metal-water mixture to criticality.

In Table 4 we show the results for k_{12} and k_{21} as determined from Equations (5), (6) and (7). Both methods predict that k_{21} is always much larger than k_{12} . The behavior of the coupling parameters with the size of the metal pit is not the same. The analytical expressions predict monotonic behavior. The ratio of neutron source method, Equation (5), predicts varying behavior depending on the concentration of the metal-water mixture.

Conclusions

The calculations reported in this paper have provided qualitative insight into the dissolver paradox which we considered to be coupled fast-thermal reactors. Each reactor in isolation is subcritical. Neutrons from the metallic pit appear to drive the metal-water mixture to the critical state. The coupling parameters were calculated in two ways. While both methods indicate that k_{21} is always much larger than k_{12} , the present analysis cannot determine which result is to be preferred. What is needed to solve this issue is a new feature in MCNP in which tallies can be flagged by the cell in which the neutrons are born.

Table 1 SAN Results

Dens.	M_pit	R _{<}	R _{>}	kb ₁	kc ₂	4πR _{<} ²	4πR _{>} ²	M_soln	M_total	V1+V2
g/cc	kg	cm	cm			cm ²	cm ²	g	g	liters
0.032	1.00	2.29693	14.0743	0.5863	0.9595	66.30	2489.22	372.07	1372.07	11.68
0.032	1.50	2.62933	13.5388	0.6692	0.9309	86.88	2303.41	330.20	1830.20	10.40
0.032	2.00	2.89395	12.9162	0.7334	0.8952	105.24	2096.43	285.58	2285.58	9.03
0.032	2.50	3.11742	12.1170	0.7866	0.8462	122.12	1845.02	234.40	2734.40	7.45
0.032	3.00	3.31275	11.2832	0.8322	0.7899	137.91	1599.84	187.67	3187.67	6.02
0.032	3.50	3.48742	10.3260	0.8725	0.7186	152.83	1339.91	141.90	3641.90	4.61
0.032	4.00	3.64615	9.1511	0.9090	0.6211	167.06	1052.34	96.22	4096.22	3.21
0.032	4.50	3.79215	8.2476	0.9414	0.5332	180.71	854.80	67.89	4567.89	2.35
0.100	1.00	2.29693	11.5452	0.5905	0.9608	66.30	1675.00	639.52	1639.52	6.45
0.100	1.50	2.62933	11.1137	0.6733	0.9200	86.88	1552.13	567.39	2067.39	5.75
0.100	2.00	2.89395	10.5695	0.7374	0.8866	105.24	1403.85	484.45	2484.45	4.95
0.100	2.50	3.11742	10.0327	0.7901	0.8423	122.12	1264.87	410.31	2910.31	4.23
0.100	3.00	3.31275	9.3764	0.8353	0.7842	137.91	1104.80	330.07	3330.07	3.45
0.100	3.50	3.48742	8.6933	0.8749	0.7174	152.83	949.69	257.43	3757.43	2.75
0.100	4.00	3.64615	7.8211	0.9107	0.6256	167.06	768.68	180.10	4180.10	2.00
0.100	4.50	3.79215	6.9792	0.9421	0.5247	180.71	612.10	119.56	4619.56	1.42
0.200	1.00	2.29693	11.0693	0.5912	0.9600	66.30	1539.75	1126.10	2126.10	5.68
0.200	1.50	2.62933	10.6365	0.6740	0.9273	86.88	1421.70	992.90	2492.90	5.04
0.200	2.00	2.89395	10.1605	0.7379	0.8880	105.24	1297.30	858.45	2858.45	4.39
0.200	2.50	3.11742	9.6218	0.7907	0.8434	122.12	1163.39	720.87	3220.87	3.73
0.200	3.00	3.31275	8.9780	0.8358	0.7848	137.91	1012.91	575.79	3575.79	3.03
0.200	3.50	3.48742	8.2767	0.8755	0.7154	152.83	860.85	439.47	3939.47	2.38
0.200	4.00	3.64615	7.5287	0.9109	0.6340	167.06	712.28	316.89	4316.89	1.79
0.200	4.50	3.79215	6.6825	0.9422	0.5306	180.71	561.16	204.32	4704.32	1.25
0.300	1.00	2.29693	10.9170	0.5914	0.9580	66.30	1497.67	1619.77	2519.77	5.45
0.300	1.50	2.62933	10.4922	0.6742	0.9266	86.88	1383.39	1428.56	2928.56	4.84
0.300	2.00	2.89395	10.0311	0.7381	0.8904	105.24	1264.47	1237.94	3237.94	4.23
0.300	2.50	3.11742	9.4829	0.7908	0.8444	122.12	1130.04	1033.53	3533.53	3.57
0.300	3.00	3.31275	8.8342	0.8362	0.7832	137.91	980.72	820.72	3820.72	2.89
0.300	3.50	3.48742	8.1445	0.8758	0.7161	152.83	833.57	625.60	4125.60	2.26
0.300	4.00	3.64615	7.3907	0.9109	0.6347	167.06	686.41	446.39	4446.39	1.69
0.300	4.50	3.79215	6.5572	0.9421	0.5324	180.71	540.32	285.77	4785.77	1.18
0.400	1.00	2.29693	10.8454	0.5919	0.9577	66.30	1478.09	2117.08	3117.08	5.34
0.400	1.50	2.62933	10.4280	0.6747	0.9269	86.88	1366.51	1869.54	3369.54	4.75
0.400	2.00	2.89395	9.9490	0.7387	0.8878	105.24	1243.85	1609.39	3609.39	4.13
0.400	2.50	3.11742	9.4131	0.7915	0.8445	122.12	1113.46	1346.74	3846.74	3.49
0.400	3.00	3.31275	8.7566	0.8367	0.7848	137.91	963.57	1064.09	4064.09	2.81
0.400	3.50	3.48742	8.0568	0.8764	0.7145	152.83	815.71	805.19	4305.19	2.19
0.400	4.00	3.64615	7.3305	0.9116	0.6367	167.06	675.27	578.78	4578.78	1.65
0.400	4.50	3.79215	6.4876	0.9431	0.5333	180.71	528.91	366.13	4866.13	1.14

Table 2. MCNP Results

Dens. [g/cc]	M-pit [kg]	ka_1	ka_1:2	ka_1:3	ka_2	ka_2:1	ka_2:3	kb_1	kb_1:2	kc_2	kc_2:1	kc_2:3
0.032	1.0	0.676	0.367	0.003	0.986	0.091	0.310	0.606	0.153	0.934	0.039	0.299
0.032	1.5	0.762	0.371	0.004	0.998	0.140	0.318	0.690	0.177	0.905	0.057	0.298
0.032	2.0	0.790	0.351	0.005	0.993	0.173	0.331	0.748	0.187	0.868	0.076	0.299
0.032	2.5	0.881	0.362	0.009	0.999	0.215	0.354	0.797	0.200	0.823	0.087	0.317
0.032	3.0	0.888	0.332	0.010	1.001	0.337	0.398	0.840	0.209	0.766	0.101	0.323
0.032	3.5	0.937	0.315	0.013	1.006	0.430	0.462	0.883	0.219	0.696	0.125	0.323
0.032	4.0	0.946	0.284	0.021	1.006	0.548	0.550	0.914	0.220	0.592	0.143	0.323
0.032	4.5	0.961	0.270	0.038	1.006	0.647	0.650	0.945	0.228	0.514	0.158	0.318
0.100	1.0	0.726	0.408	0.007	1.003	0.105	0.393	0.606	0.153	0.945	0.058	0.370
0.100	1.5	0.805	0.396	0.009	0.997	0.163	0.410	0.690	0.177	0.912	0.073	0.369
0.100	2.0	0.821	0.363	0.013	0.998	0.217	0.429	0.748	0.187	0.873	0.090	0.384
0.100	2.5	0.900	0.360	0.014	1.009	0.283	0.466	0.797	0.200	0.818	0.107	0.388
0.100	3.0	0.912	0.320	0.015	1.000	0.359	0.500	0.840	0.209	0.772	0.124	0.401
0.100	3.5	0.943	0.311	0.020	1.004	0.452	0.560	0.883	0.219	0.698	0.141	0.395
0.100	4.0	0.955	0.282	0.032	1.007	0.556	0.654	0.914	0.220	0.619	0.166	0.392
0.100	4.5	0.957	0.255	0.049	1.006	0.665	0.767	0.945	0.228	0.511	0.172	0.373
0.200	1.0	0.700	0.394	0.008	1.003	0.101	0.416	0.606	0.153	0.953	0.057	0.397
0.200	1.5	0.770	0.383	0.013	1.002	0.142	0.428	0.690	0.177	0.918	0.079	0.399
0.200	2.0	0.860	0.382	0.011	1.007	0.208	0.448	0.748	0.187	0.882	0.094	0.406
0.200	2.5	0.871	0.342	0.011	0.997	0.268	0.473	0.797	0.200	0.841	0.111	0.407
0.200	3.0	0.910	0.326	0.019	1.001	0.349	0.523	0.840	0.209	0.781	0.127	0.416
0.200	3.5	0.936	0.309	0.027	1.002	0.431	0.588	0.883	0.219	0.715	0.143	0.418
0.200	4.0	0.963	0.286	0.036	1.012	0.547	0.674	0.914	0.220	0.620	0.161	0.407
0.200	4.5	0.967	0.254	0.050	1.007	0.652	0.776	0.945	0.228	0.526	0.170	0.394
0.300	1.0	0.720	0.399	0.007	1.015	0.105	0.410	0.606	0.153	0.965	0.060	0.400
0.300	1.5	0.781	0.385	0.010	1.013	0.152	0.428	0.690	0.177	0.910	0.070	0.407
0.300	2.0	0.847	0.371	0.011	1.005	0.206	0.453	0.748	0.187	0.892	0.093	0.404
0.300	2.5	0.875	0.341	0.016	1.020	0.287	0.488	0.797	0.200	0.852	0.111	0.422
0.300	3.0	0.908	0.322	0.020	1.006	0.343	0.532	0.840	0.209	0.791	0.133	0.421
0.300	3.5	0.972	0.305	0.026	1.020	0.441	0.601	0.883	0.219	0.712	0.142	0.424
0.300	4.0	0.953	0.279	0.032	1.009	0.540	0.668	0.914	0.220	6.331	0.163	0.415
0.300	4.5	0.966	0.254	0.048	1.003	0.632	0.777	0.945	0.228	0.526	0.170	0.394
0.400	1.0	0.692	0.380	0.007	1.013	0.096	0.411	0.606	0.153	0.965	0.055	0.400
0.400	1.5	0.815	0.391	0.011	1.021	0.168	0.429	0.690	0.177	0.941	0.078	0.411
0.400	2.0	0.843	0.368	0.014	1.021	0.207	0.453	0.748	0.187	0.901	0.092	0.406
0.400	2.5	0.891	0.356	0.015	1.011	0.267	0.486	0.797	0.200	0.853	0.109	0.421
0.400	3.0	0.912	0.329	0.021	1.021	0.346	0.540	0.840	0.209	0.789	0.127	0.417
0.400	3.5	0.943	0.307	0.026	1.015	0.432	0.587	0.883	0.219	0.728	0.145	0.427
0.400	4.0	0.944	0.277	0.033	1.007	0.524	0.664	0.914	0.220	0.634	0.157	0.410
0.400	4.5	0.988	0.261	0.051	1.013	0.640	0.769	0.945	0.228	0.540	0.174	0.401

Table 3. Coupling Parameters from Power Ratio

Dens. [g/cc]	M-pit [kg]	S ₁	S ₂	S ₁ /S ₂	ka_1	ka_2	k ₁₂	k ₂₁
0.032	1.0	2.8161E-02	3.1701E-01	8.8833E-02	0.606	0.934	0.035	0.747
0.032	1.5	4.5184E-02	3.0529E-01	1.4800E-01	0.690	0.905	0.046	0.641
0.032	2.0	6.1079E-02	2.8564E-01	2.1383E-01	0.748	0.868	0.054	0.615
0.032	2.5	8.2295E-02	2.6190E-01	3.1422E-01	0.797	0.823	0.064	0.564
0.032	3.0	1.0834E-01	2.3869E-01	4.5389E-01	0.840	0.766	0.073	0.516
0.032	3.5	1.3905E-01	2.0547E-01	6.7674E-01	0.883	0.696	0.079	0.448
0.032	4.0	1.7700E-01	1.6269E-01	1.0880E+00	0.914	0.592	0.093	0.375
0.032	4.5	2.1262E-01	1.2686E-01	1.6760E+00	0.945	0.514	0.093	0.290
0.100	1.0	2.9384E-02	3.2073E-01	9.1616E-02	0.606	0.945	0.036	0.600
0.100	1.5	4.6343E-02	3.0163E-01	1.5364E-01	0.690	0.912	0.048	0.571
0.100	2.0	6.4629E-02	2.8215E-01	2.2906E-01	0.748	0.873	0.058	0.554
0.100	2.5	8.5407E-02	2.6208E-01	3.2588E-01	0.797	0.818	0.066	0.557
0.100	3.0	1.1248E-01	2.3203E-01	4.8476E-01	0.840	0.772	0.078	0.470
0.100	3.5	1.3983E-01	2.0182E-01	6.9285E-01	0.883	0.698	0.081	0.436
0.100	4.0	1.7690E-01	1.6183E-01	1.0931E+00	0.914	0.619	0.094	0.349
0.100	4.5	2.1667E-01	1.2127E-01	1.7867E+00	0.945	0.511	0.099	0.274
0.200	1.0	2.7560E-02	3.2189E-01	8.5619E-02	0.606	0.953	0.034	0.549
0.200	1.5	4.1573E-02	3.0544E-01	1.3611E-01	0.690	0.918	0.042	0.599
0.200	2.0	6.2727E-02	2.8723E-01	2.1839E-01	0.748	0.882	0.055	0.540
0.200	2.5	8.1455E-02	2.6299E-01	3.0973E-01	0.797	0.841	0.063	0.514
0.200	3.0	1.0702E-01	2.3675E-01	4.5204E-01	0.840	0.781	0.072	0.485
0.200	3.5	1.3682E-01	2.0345E-01	6.7250E-01	0.883	0.715	0.078	0.424
0.200	4.0	1.7440E-01	1.6703E-01	1.0441E+00	0.914	0.620	0.089	0.364
0.200	4.5	2.1217E-01	1.2555E-01	1.6899E+00	0.945	0.526	0.093	0.281
0.300	1.0	2.7939E-02	3.2624E-01	8.5639E-02	0.606	0.965	0.034	0.409
0.300	1.5	4.2543E-02	3.0960E-01	1.3741E-01	0.690	0.910	0.043	0.656
0.300	2.0	6.0039E-02	2.8725E-01	2.0901E-01	0.748	0.892	0.053	0.517
0.300	2.5	8.4723E-02	2.6833E-01	3.1574E-01	0.797	0.852	0.064	0.469
0.300	3.0	1.0812E-01	2.4017E-01	4.5018E-01	0.840	0.791	0.072	0.464
0.300	3.5	1.3956E-01	2.0896E-01	6.6738E-01	0.883	0.712	0.142	0.424
0.300	4.0	1.7113E-01	1.6995E-01	1.0069E+00	0.914	0.633	0.086	0.364
0.300	4.5	2.0736E-01	1.2986E-01	1.5968E+00	0.945	0.526	0.088	0.297
0.400	1.0	2.7030E-02	3.2676E-01	8.2721E-02	0.606	0.965	0.033	0.423
0.400	1.5	4.4556E-02	3.1180E-01	1.4290E-01	0.690	0.941	0.044	0.414
0.400	2.0	6.1533E-02	2.9325E-01	2.0983E-01	0.748	0.901	0.053	0.472
0.400	2.5	8.0844E-02	2.6851E-01	3.0108E-01	0.797	0.853	0.061	0.487
0.400	3.0	1.0711E-01	2.4403E-01	4.3892E-01	0.840	0.789	0.070	0.481
0.400	3.5	1.3516E-01	2.1042E-01	6.4233E-01	0.883	0.728	0.075	0.423
0.400	4.0	1.6778E-01	1.7511E-01	9.5814E-01	0.914	0.634	0.082	0.382
0.400	4.5	2.0632E-01	1.3110E-01	1.5738E+00	0.945	0.540	0.087	0.292

Table 4. Comparison of Coupling Parameters Determinations

Dens. [g/cc]	M-pit [kg]	k_{12} Eq (5)	k_{12} Eq.(7)	k_{21} Eq. (5)	k_{21} Eq. (6)
0.032	1.0	0.035	0.007	0.747	0.789
0.032	1.5	0.046	0.011	0.641	0.746
0.032	2.0	0.054	0.016	0.615	0.702
0.032	2.5	0.064	0.023	0.564	0.655
0.032	3.0	0.073	0.031	0.516	0.601
0.032	3.5	0.079	0.043	0.448	0.538
0.032	4.0	0.093	0.062	0.375	0.452
0.032	4.5	0.093	0.082	0.290	0.388
0.100	1.0	0.036	0.011	0.600	0.799
0.100	1.5	0.048	0.018	0.571	0.752
0.100	2.0	0.058	0.025	0.554	0.706
0.100	2.5	0.066	0.034	0.557	0.651
0.100	3.0	0.078	0.045	0.470	0.606
0.100	3.5	0.081	0.060	0.436	0.540
0.100	4.0	0.094	0.081	0.349	0.472
0.100	4.5	0.099	0.108	0.274	0.386
0.200	1.0	0.034	0.012	0.549	0.806
0.200	1.5	0.042	0.019	0.599	0.757
0.200	2.0	0.055	0.027	0.540	0.713
0.200	2.5	0.063	0.036	0.514	0.669
0.200	3.0	0.072	0.049	0.485	0.613
0.200	3.5	0.078	0.065	0.424	0.553
0.200	4.0	0.089	0.086	0.364	0.473
0.200	4.5	0.093	0.115	0.281	0.397
0.300	1.0	0.034	0.013	0.409	0.816
0.300	1.5	0.043	0.020	0.656	0.751
0.300	2.0	0.053	0.027	0.517	0.721
0.300	2.5	0.064	0.037	0.469	0.678
0.300	3.0	0.072	0.050	0.464	0.620
0.300	3.5	0.142	0.067	0.424	0.550
0.300	4.0	0.086	0.088	0.364	0.483
0.300	4.5	0.088	0.118	0.297	0.397
0.400	1.0	0.033	0.013	0.423	0.816
0.400	1.5	0.044	0.020	0.414	0.776
0.400	2.0	0.053	0.027	0.472	0.728
0.400	2.5	0.061	0.037	0.487	0.679
0.400	3.0	0.070	0.050	0.481	0.619
0.400	3.5	0.075	0.067	0.423	0.563
0.400	4.0	0.082	0.088	0.382	0.484
0.400	4.5	0.087	0.119	0.292	0.408

References

1. W. A. Reardon and F. R. Czerniejewski, "A Study of Idealized Plutonium Metal Dissolvers and the "Always Safe" Condition," *Transactions American Nuclear Society*, **6**,170 (1963).
2. R. Avery, *Proceedings of the Second United Nations International Conference on Peaceful Uses of Atomic Energy, Geneva, 1958* United Nations, Geneva, (1958).
3. W. W. Engle, Jr., "A User's Manual for ANISN, A One-Dimensional Discrete Ordinates Transport Code with Anisotropic Scattering, K-1693, Union Carbide Corporation, Oak Ridge, TN, (1967)
4. J. G. Briesmeister, Ed., "MCNP - A General Monte Carlo Code for Neutron, Photon and Electron Transport, Version 3A/3B/4," Los Alamos National Laboratory, Los Alamos, NM, LA-7396-M, (1986/Rev. 1988 and 1991)

This work was performed under the auspices of the U.S. Department of Energy by Lawrence Livermore National Laboratory under contract No. W-7405-Eng-48.

END

**DATE
FILMED**

9 / 15 / 193

